

Electron Scattering from Nuclear Targets
and Quark Distributions in Nuclei*

A. Bodek, N. Giokaris
Department of Physics and Astronomy
University of Rochester
Rochester, N.Y. 14627, USA

W. B. Atwood, D. H. Coward and D. J. Sherden
Stanford Linear Accelerator Center
Stanford University
Stanford, CA 94305, USA

D. L. Dubin, J. E. Elias,¹ J. I. Friedman, H. W. Kendall
J. S. Poucher,² E. M. Riordan³ and M. R. Sogard⁴
Physics Department and Laboratory for Nuclear Science
Massachusetts Institute of Technology
Cambridge, MA 02139, USA

Abstract

We have measured the deep inelastic electromagnetic structure functions of steel, deuterium and hydrogen nuclei using the high energy electron beam at the Stanford Linear Accelerator Center. The ratio of the structure functions of steel and deuterium cannot be understood simply by corrections due to Fermi motion effects. The data indicate that the quark momentum distributions in the nucleon become distorted in the nucleus. Our results are consistent with recent measurements with high energy muon beams.

(Submitted to Physical Review Letters)

*Work supported in part by the Department of Energy contracts DE-AC03-76SF00515, DE-AC02-76ER13065 and DE-AC02-03069.

1. Present Address: Fermilab, Batavia, IL 60510.
2. Present Address: Bell Labs., Holmdel, NJ 07733.
3. Present Address: Cheshire Books, 514 Bryant St., Palo Alto, CA 94301.
4. Present Address: GCA Corp., 209 Burlington Rd., Bedford, MA 07130.

The structure functions of the neutron (F_2^{en}) and proton (F_2^{ep}) have been determined from deep-inelastic electron scattering experiments^{1,2} using hydrogen and deuterium targets. Within the quark-parton model, these structure functions, at sufficiently large momentum transfers, determine the quark momentum distributions in the nucleon. Detailed studies of the atomic weight dependence of inelastic electron scattering cross sections^{2,3} have concentrated primarily in the low x , and low Q^2 region where the application of the quark-parton model is not valid, and where other effects such as nuclear shadowing⁴ may be important. The atomic weight dependence in the large x and large Q^2 region has not been studied until recently.

Recent results⁵ from the European Muon Collaboration⁶ (EMC) indicate that there is a significant difference between the nucleon structure functions extracted from data obtained from muon-steel and muon-deuterium scattering experiments. This difference exhibits a trend which is opposite from that expected from Fermi motion effects.⁷ Recent bag model calculations,⁸ motivated by these recent results, suggest that the quark distributions in a nucleon become distorted in a nucleus via mechanisms such as six quark bag states.

In this letter we report an observation of a significant difference between the structure functions of steel and deuterium extracted from deep inelastic electron scattering data taken at the Stanford Linear Accelerator Center (SLAC). Such a comparison is important not only as a search for changes in the quark structure of nucleons in nuclei as a basic physics question, but also because all present high statistics muon and neutrino high energy scattering experiments utilize heavy nuclear targets. The nuclear corrections^{7,8} mentioned above can affect the interpretation of the structure function results when compared to the predictions of Quantum Chromodynamics (QCD), especially when data from different target nuclei have been combined in such a comparison.

The SLAC experiment^{9,10} was designed to measure deep inelastic electron scattering from hydrogen and deuterium at large values of x and Q^2 in order to extract the proton and neutron structure functions. The structure functions were extracted using hydrogen and deuterium targets and a steel empty target replica. Results on the ratio of neutron and proton structure functions were reported⁹ in 1974. A later comprehensive article¹⁰ described the experiment in detail and examined the scaling of the neutron and proton structure functions in the SLAC energy range. We have recently analysed the empty target data in order to compare the steel and deuterium structure functions. We comment briefly on those points of the experiment related to this comparison.

Differential cross sections for the scattering of electrons from hydrogen, deuterium and steel were measured with the SLAC 8-GeV spectrometer at laboratory scattering angles (θ) of 15° , 19° , 26° and 34° . At each angle, measurements were made over a range of scattered electron energy E' for several values of incident electron energy E between 8.7 and 20 GeV. The electron beam passed through 14 cm long liquid hydrogen and liquid deuterium targets with walls made of 0.001" thick stainless steel.¹¹ The empty target contributions were measured using a steel empty target replica with 0.007" thick walls, chosen so that the amount of radiator in the steel target replica was nearly the same as that for the full targets. Thus the radiative corrections for full and empty target data were essentially identical.^{12,13} The rates measured with the empty target replica were divided by the ratio of the wall thicknesses (7.0) before subtraction from the full target rates. The measurements with hydrogen, deuterium and empty replica targets were interspersed to minimize systematic errors in the ratios. In the current analysis, we have used the data from the steel empty target replica to extract the structure functions for steel.

The data lie in the kinematic range $4 < Q^2 < 21$ (GeV/c)² and $0.25 < x < 0.90$, for $W \geq 1.8$ (GeV/c)². The mass W of the unobserved hadronic final state is defined by $W^2 = M^2 + 2M\nu - Q^2$, where M is the mass of the proton, $\nu = E - E'$ is the energy transfer and $Q^2 = -q^2 = 4EE'\sin^2(\theta/2)$ is the invariant square of the four momentum transfer. We define the scaling variables $x = Q^2/2M\nu = 1/\omega$, and $\xi = 2x/(1+\sqrt{1+4M^2x^2/Q^2})$. Within the quark-parton model, the x (or ξ) dependence of the structure functions reflects the momentum distribution of the quarks in the nucleon. The variable ξ includes finite Q^2 target mass corrections¹⁴ ($\xi=x$ in the large Q^2 limit).

The structure functions W_1 and W_2 which are defined here per nucleon are related to the differential cross sections in the usual form

$$\frac{d^2\sigma}{d\Omega dE} = \sigma_M [W_2(Q^2, x) + 2W_1(Q^2, x) \tan^2 \frac{\theta}{2}]$$

where σ_M is the Mott cross section. The ratio of W_2 to W_1 is related to $R = \sigma_L/\sigma_T$, the ratio of the cross sections for absorption of longitudinal and transverse virtual photons, by the expression $W_2/W_1 = (1+R)/(1+Q^2/4M^2x^2)$. We report here on σ_{Fe}/σ_{D_2} , the ratio of the differential cross sections per nucleon for nucleons bound in a steel nucleus and nucleons bound in the deuteron. - Equality of R for a nucleon bound in steel and for a nucleon bound in the deuteron would allow interpretation of σ_{Fe}/σ_{D_2} as the structure function ratio $\nu W_2^{Fe}/\nu W_2^{D_2} = F_2^{Fe}/F_2^{D_2}$ where F_2 is the structure function associated with W_2 that exhibits approximate scaling.

The measured raw cross section ratios σ_{Fe}/σ_{D_2} were corrected for the small acceptance difference between the steel and deuterium targets.¹⁵ A small correction (1% to 3%) was applied for the neutron excess in steel (using fits to neutron and proton data¹⁰) such that σ_{Fe} as reported here is the cross section per nucleon in a hypothetical steel nucleus with equal numbers of

neutrons and protons. In addition, a small correction was applied for the small difference in the radiative corrections for steel and deuterium targets. The radiative corrections, calculated using the method of Mo and Tsai¹⁶ as described in detail in Stein et al.² changed the $\sigma_{\text{Fe}}/\sigma_{\text{D}_2}$ ratio by less than 1%. The calculation included the contribution of the radiative tails from the elastic scattering from steel and deuterium nuclei (negligible in our range of momentum transfers) as well as contributions from quasielastic and inelastic processes.

Values of $\sigma_{\text{Fe}}/\sigma_{\text{D}_2}$ as functions of x and ξ are given in Table 1 and shown in Figure 1. The values were obtained by calculating the ratios at all kinematic points with $W \geq 1.8 \text{ GeV}/c^2$ and forming weighted averages¹⁷ over small intervals in x or ξ ($\Delta x = 0.05$). The random errors arising from counting statistics dominate the typically 1% error in the cross sections obtained by adding in quadrature the errors from random fluctuations (e.g. flux monitors, liquid target densities and rate dependent effects). Only random errors are shown in the errors of the points in Figure 1. Most systematic errors in the cross sections (solid angle, incident and scattered electron energy calibration, monitor calibration and most uncertainties in the radiative corrections) cancel in the ratio $\sigma_{\text{Fe}}/\sigma_{\text{D}_2}$. The number of nucleons/cm² in the steel empty target replica was measured to an accuracy of $\pm 0.8\%$ by weighing sections cut out of the target in the region which was traversed by the beam and measuring the areas with a planimeter. The number of nucleons/cm² in the liquid deuterium target was determined to an accuracy¹⁰ of $\pm 0.8\%$. We estimate an overall systematic error of $\pm 1.1\%$ in the $\sigma_{\text{Fe}}/\sigma_{\text{D}_2}$ ratio. The systematic error in this ratio from radiative corrections is estimated to be less than 1%. The electron data show a significant x dependence difference between the steel and deuterium

cross sections. The observed effect is consistent with recent results obtained with muons by the EMC collaboration⁵.

In view of the small statistical and systematic errors we conclude that the difference between the steel and deuterium cross sections is due to nuclear effects. The effects of Fermi motion of the nucleons in the steel nucleus and in the deuteron have been calculated by Bodek and Ritchie⁷ using an extension of the original calculations of Atwood and West¹⁸ for the deuteron. The expected contribution from Fermi motion effects to the ratio of steel to deuterium cross sections is shown in Figure 1. The cross sections for steel were expected to be larger than those for the deuteron for $x > 0.5$, because the momentum spread of the wave function for nucleons bound in steel is larger than the momentum spread of the deuteron wave function. The behavior of the data for $x < 0.80$ is opposite to that expected from Fermi motion. However, the data suggest that for $x > 0.8$ the effects of Fermi motion become dominant.

The variation of the data as shown in Figure 1 cannot, in present models, be explained in terms of nuclear shadowing. Nuclear shadowing is expected to be important only at small values of x and Q^2 where deviations from the quark parton model are expected due to effects such as the coupling between the photon and vector mesons⁴ (or "higher twist" effects in the language of QCD). Radiative corrections^{2,16} are well understood and are not expected to result in the observed variation with x .

Within the quark-parton model, the x distributions of the structure functions reflect the momentum distributions of the quarks in the nucleon. Thus the data indicate that the quark momentum distributions in the nucleon become distorted in the presence of other nucleons in the nucleus. In view of these results, we have begun the further analysis of data from SLAC

experiment E49B¹⁹ in which an aluminum empty target was used and which covered a kinematic region extending to considerably lower values of x than those reported here. The comparison of aluminum and deuterium data will be reported in a future communication.

In summary, the data indicate significant distortions in the structure functions of nucleons bound in steel which cannot be attributed to Fermi momentum smearing. It has been suggested⁸ that similar distortions are small in the deuteron because of its large size. Experimental support for this suggestion comes from the consistency of the ratio of $d(x)$ and $u(x)$ quark distributions in the nucleon extracted from deep inelastic electron scattering experiments¹ on hydrogen and deuterium (i.e. from $F_2^{\text{en}}/F_2^{\text{ep}}$) and the same quantity extracted from neutrino and antineutrino experiments on hydrogen.²⁰

We wish to express our gratitude and appreciation to all members of the Stanford Linear Accelerator Center. We thank Ron Sax and Mark Barnett from SLAC, Jim Schlereth from Argonne and Harald Johnstad from Fermilab for their help in recovering the E87 data from old IBM tapes. This work was supported in part by Department of Energy contracts DE-AC02-76ER13065 (Rochester), DE-AC02-03069 (MIT) and DE-AC03-76SF00515 (SLAC).

References

1. A. Bodek et al., Phys. Lett. 30, 1087 (1973); J. S. Poucher et al., Phys. Rev. Lett. 32, 118 (1974); A. Bodek et al., Phys. Lett. 51B, 417 (1974); W. B. Atwood et al., Phys. Lett. 64B, 479 (1976); A. Bodek et al., Phys. Rev. D20, 1471 (1979).
2. S. Stein et al., Phys. Rev. D12, 1884 (1975).
3. W. R. Ditzler et al., Phys. Lett. 57B, 201 (1975); J. Eickmeyer et al., Phys. Rev. Lett. 36, 289 (1976); J. Bailey et al., Nucl. Phys. B151, 367 (1979); G. Huber et al., Z. Phys. C2, 279 (1979); J. Franz et al., Z. Phys. C10, 105 (1979); M. May et al., Phys. Rev. Lett. 35, 407 (1975); M. Miller et al., Phys. Rev. D24, 1 (1981).
4. G. Grammer and J. D. Sullivan, "Nuclear Shadowing of Electromagnetic Processes", in "Electromagnetic Interactions of Hadrons", Vol. 2, p.195; Ed. A. Donnachie and G. Shaw, Plenum Press, 1978.
5. J. J. Aubert et al., CERN-EP/83-14 (submitted to Phys. Lett. B).
6. J. J. Aubert et al., Phys. Lett. 105B, 315, 322 (1981).
7. A. Bodek and J. L. Ritchie, Phys. Rev. D23, 1070 (1981); D24, 1400 (1981).
8. R. L. Jaffe, Phys. Rev. Lett. 50, 228 (1983).
9. A. Bodek et al., Phys. Lett. 51B, 417 (1974).
10. SLAC experiment E87 referred to as experiment B in A. Bodek et al., Phys. Rev. D20, 1471 (1979).
11. Type 347 stainless steel nominal density 8.0 g/cm^3 , radiation length = 1.74 cm, mean $A = 55.13$, mean $Z = 25.69$, average composition mainly 66.8% Fe($A=55.8$), 18.7% Cr($A=52$), 11.3% Ni($A=58.7$), 1.7% Mn($A=54.9$). Note that the number of nucleons/ cm^2 was directly measured (see text).
12. A. Bodek, Nucl. Inst. and Meth. 109, 603 (1973).
13. In units of 10^{-2} radiation lengths, the value used for the average amount of radiator before scattering was 1.122 and 1.065 for deuterium and steel,

- respectively. The average amounts after the scattering at angles of 15°, 19°, 26° and 34° were 1.558, 1.552, 1.537 and 1.513 for deuterium and 1.584, 1.607, 1.662 and 1.755 for steel, respectively.
14. O. Nachtmann, Nucl. Phys. B63, 237 (1973); H. Georgi and H. D. Politzer, Phys. Rev. D14, 1829 (1976).
 15. The acceptance for the empty target was smaller than the acceptance for the full target by 0.4%, 0.5%, 0.7% and 1.1% for data taken at 15°, 19°, 26° and 34°, respectively.
 16. L. W. Mo and Y. S. Tsai, Rev. Mod. Phys. 41, 205 (1969), L. C. Maximon, Rev. Mod. Phys. 41, 193 (1969).
 17. A. Bodek, Nucl. Inst. and Meth. 117, 613 (1974), 150, 367 (1978); A. Bodek, SLAC-TN-74-2, 1974 (unpublished).
 18. G. B. West, Ann. Phys. (NY) 74, 464 (1972); W. B. Atwood and G. B. West, Phys. Rev. D7, 773 (1973).
 19. A. Bodek et al., Phys. Rev. Lett. 30, 1087 (1973), SLAC experiment E49B referred to as experiment A in Ref. 10.
 20. G. R. Farrar et al., Phys. Lett. 69B, 112 (1977); P. Allen et al., Phys. Lett. 103B, 71 (1981); F. Eisele in Proceedings of the 21st International Conference on High Energy Physics p. C3-337 (1982), P. Petiau and M. Porneut eds.; see also J. Hanlon et al., Phys. Rev. Lett. 45, 1817 (1980).

Figure Caption

Figure 1: $\sigma_{\text{Fe}}/\sigma_{\text{D}_2}$ versus x . Only random errors are shown. All data for $W \geq 1.8$ GeV are included. The data have been corrected for the small neutron excess in steel. The data have not been corrected for Fermi motion effects. The effect with Fermi motion corrections is much larger (see Table 1). The curve indicates the expected ratio if Fermi motion effects were the only effects present (Ref. 7). Recent data from muon scattering (EMC, Ref. 5) are shown for comparison. The systematic error for the electron data is estimated at $\pm 1.1\%$. The systematic error in the muon data (EMC) is $\pm 1.5\%$ at $x = 0.35$ and increases to $\pm 6\%$ for the points at $x = 0.05$ and $x = 0.65$.

Table Caption

Table 1: $\sigma_{\text{Fe}}/\sigma_{\text{D}_2}$ as a function of x and ξ . The ratio expected from Fermi motion is from Ref. 7. The data have been corrected for the small neutron excess in steel, and have not been corrected for Fermi motion effects. In order to correct for Fermi motion, the $\sigma_{\text{Fe}}/\sigma_{\text{D}_2}$ ratios should be divided by the numbers in column 4. The mean Q^2 is in $(\text{GeV}/c)^2$.

Table 1

x, or ξ	mean Q^2 (x bins)	$\sigma_{\text{Fe}}/\sigma_{\text{D}_2}$ (x bins)	Fermi Motion	$\sigma_{\text{Fe}}/\sigma_{\text{D}_2}$ (ξ bins)
.25	3.3	1.165±.106	0.976	1.165±.106
.30	7.2	0.951±.063	0.976	0.951±.063
.35	6.4	0.989±.017	0.978	0.986±.017
.40	7.1	0.979±.023	0.980	0.975±.018
.45	7.2	0.952±.017	0.989	0.943±.018
.50	7.6	0.933±.019	1.000	0.918±.018
.55	7.6	0.907±.020	1.011	0.897±.015
.60	6.0	0.876±.016	1.034	0.855±.017
.65	7.8	0.870±.017	1.069	0.871±.022
.70	9.7	0.885±.027	1.142	0.931±.034
.75	11.4	0.934±.041	1.262	0.931±.047
.80	12.8	0.936±.054	1.458	0.975±.083
.85	17.0	1.069±.099	1.746	1.204±.159
.90	19.3	1.162±.255	2.021	--- ---

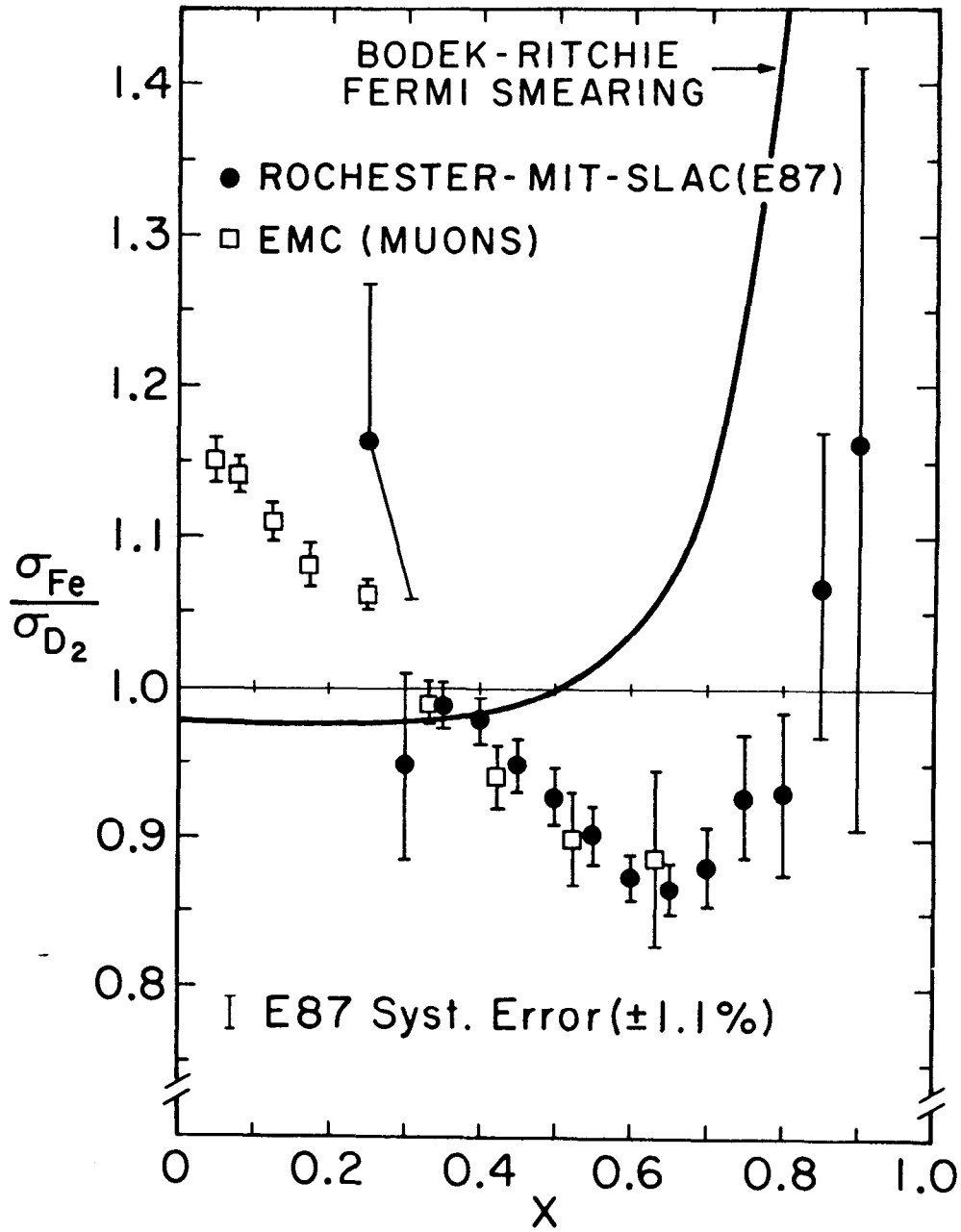


Fig. 1